Black Hole Winds at All Scales
Proceedings IAU Symposium No. 378, 2024
G. Bruni, M. Diaz Trigo, S. Laha & K. Fukumura, eds.
doi:10.1017/S1743921323002867

Updated Calculations of the Spectral-Line Radiation Force & Mass-Loss Rates for AGN Outflows

Aylecia S. Lattimer and Steven Cranmer

Department of Astrophysical & Planetary Sciences, Laboratory for Atmospheric and Space Physics, University of Colorado, Boulder, CO 80309, USA
email: aylecia.lattimer@colorado.edu
email: Steven.Cranmer@lasp.colorado.edu

Abstract. Photon-driven flows have been studied for almost a century, and a quantitative description of the radiative forces on atoms and ions is important for understanding a wide variety of systems, including active galactic nuclei (AGN). The colloquially-termed "radiation pressure" of line-driven winds plays an important role in driving outflows in these environments. Quantifying the associated forces is crucial to understanding how these flows enable interactive mechanisms within these environments, such as AGN feedback. Here we provide new calculations of the dimensionless line strength parameter due to radiation driving. For representative AGN, we calculate the photoionization balance at each step along the line of sight (LOS) to the proposed wind-launching region above the accretion disk. We then use a recently compiled database of approximately 5.6 million spectral lines to compute the strength of the line-driving force on the gas and the mass-loss rates resulting from these outflows. We also introduce a "shielding factor that increases the magnitude of the accretion disk column density prior to the launch radius. This shielding factor simulates a proposed inner failed wind region that is thought to shield the outflowing gas from becoming over-ionized by the central source. We also revisit and formalize the role of the commonly-used ionization parameter in setting the properties of the accelerating gas.

Keywords. AGN outflows, radiative processes, atomic physics

1. Introduction

Active Galactic Nuclei (AGN) are believed to be powered by accretion onto a supermassive black hole (SMBH), and quantifying and understanding the associated mass and energy flows are crucial to understanding the observed properties of quasars, blazars, Seyfert, and radio galaxies, as well as how these objects evolve and interact with their surroundings. These outflows are suspected of influencing star formation rates far beyond the small-scale size of the AGN itself. This long-range"feedback" is likely responsible for producing several known correlations between the SMBH mass and a range of large-scale properties of the host galaxy and intergalactic medium (Magorrian et al. 1998; Silk & Rees 1998; Cavaliere et al. 2002; Ostriker et al. 2010; Fabian 2012; King & Pounds 2015; Hopkins et al. 2016; Harrison et al. 2018).

There are multiple possible mechanisms to accelerate AGN winds. It is likely that some combination of effects may be responsible for accelerating various features. However, this work focuses on radiative driving as a possible mechanism for launching and sustaining AGN outflows (Giustini & Proga 2019). This is often referred to as "radiation pressure," where the force of radiation from the spectral lines acts on the material of the outflow.

The extremely large number of spectral lines in any given ion has a dominant effect on this pressure on the flow material (Castor 1974; Castor et al. 1975). The absorption and re-emission of photons in a spectral line results in a radial transfer of momentum, driving a wind outward from the source, in this case an AGN. This type of driving has been suggested to occur in the broad absorption line (BAL) region of AGN, where the blueshift of the spectral lines suggest that outflow velocities can reach up to $0.2c$. Line-driven disk winds are a promising hydrodynamical scenario for these outflows, due in part to the large number of strong resonance lines present in the spectra of many BAL quasars (BALQSOs; Murray et al. 1995; Proga et al. 2000; Proga 2007; Risaliti & Elvis 2010; Higginbottom et al. 2014; Nomura et al. 2016; Zhu et al. 2022).

However, in order for line-driving to launch and maintain an outflow from the accretion disk, the material must be relatively lowly-ionized. As more of the wind material becomes highly ionized, such as that in close proximity to the black hole, there are fewer spectral lines present for the radiation from the source to act upon (Higginbottom et al. 2014). A proposed solution to this issue is a so-called "failed wind" near the interior of the accretion disk, which acts to shield the outer material from becoming over-ionized (see, for example, Proga et al. 2000, Proga & Kallman 2004).

In this work, we provide new calculations of the dimensionless line strength parameter due to radiation driving, as well as explore the importance of the previously mentioned failed wind in launching and maintaining a line-driven disk wind. We also revisit and formalize the role of the commonly-used ionization parameter in setting the properties of the accelerating gas.

2. Overview

Since a complete tabulation of the line force requires the inclusion of as many lines as possible, the atomic line data used in this work was retrieved from a variety of sources. Multiple atomic databases were used to fill in any gaps in the available data wherever possible. Databases used include the National Institute of Standards and Technology (NIST; Kramida et al. 2018), version 10.0 of the CHIANTI database (Dere et al. 1997; Del Zanna et al. 2021), the database of lines used by the radiative transfer code CMFGEN (Hillier 1990; Hillier & Miller 1998; Hillier & Lanz 2001), the Opacity Project's TOPbase (Cunto & Mendoza 1992; Cunto et al. 1993), and the XSTAR database (Mendoza et al. 2021). For the AGN central sources considered here the more highly ionized states of each element become increasingly important. Therefore, where available, all ionization states for all elements up to Zn ($Z = 30$) were included. The CHIANTI and CMFGEN databases additionally include both theoretical and observed spectral line data. For the sake of completeness, the compiled line list is comprised of both theoretical (where applicable) and observed transitions. The final line list contained data for 5,671,602 spectral lines.

The core aim of this work is to determine the usefulness of the ionization parameter ξ in determining the ionization balance of the wind material. Since our goal is to model line forces for a wide range of possible AGN environments and outflow features, we vary the basic properties of the AGN and the absorbed line of sight in order to reveal the full range of possible regimes. The initial input parameters of each model include mass of the black hole, Eddington ratio, wind mass flux and speed, wind launch radius, viewing angle, and shielding factor, which enhances the hydrogen number density prior to the launch radius. To determine the efficacy of the ionization parameter ξ, we calculate the complete ionization balance at every step along the modeled line of sight. The model geometry used is shown in Figure 1. The initial spectral energy distribution (SED) is given by the python module QSOSED (`https://github.com/arnauqb/qsosed`). We calculate the initial thermal equilibrium and ionization balance from the SED at the first radial step, defined as the radius of the corona, R_{cor}.

https://doi.org/10.1017/S1743921323002867 Published online by Cambridge University Press

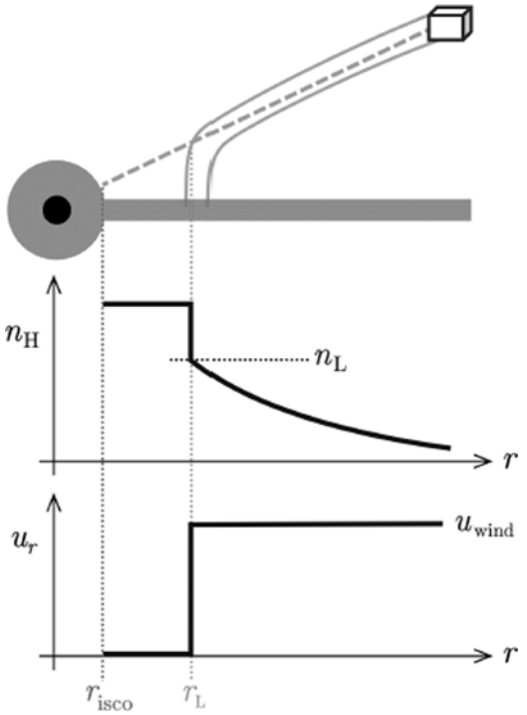

Figure 1. Modeled radial line-of-sight geometry at a given angle above the disk, shown with representative versions of the hydrogen number density n_H and radial flow speed u_r. Dashed line shows the modeled line of sight to the parcel of gas. The radius of the innermost stable circular orbit and launch radius of the wind are denoted by r_{isco} and r_L respectively. The curvature of the flux tube is shown for completeness, but was not considered in this work.

There are five processes that need to be accounted for in this calculation: collisional ionization (CI_i), autoionization (AI_i), photoionization (PI_i), radiative recombination (RR_{i+1}), and dielectric recombination (DI_{i+1}). We do not include three-body recombination, as it generally does not represent a significant contribution to the ionization balance except in the high-density limit, which the AGN environments considered here traditionally do not experience (see, e.g., Rees et al. 1989). The five rates considered are given in units of s^{-1}. For a time steady case, we can write the ionization balance as

$$\frac{n_{i+1}}{n_i} = \frac{CI_i + AI_i + PI_i}{RR_{i+1} + DR_{i+1}}. \tag{1}$$

Using the calculated ionization balance, the luminosity is then recalculated according to the attenuation of the SED due to the intervening material. These calculations are then repeated for each radial step along the line of sight grid.

Because the luminosity is comprised of three separate components, the hot corona, the warm comptonising region, and the cool disk, two limiting cases of the attenuation were considered: attenuation of only the corona component of the luminosity along the line of sight, and equal attenuation of all three luminosity components along the line of sight. These two cases are used to limit the behavior of the force multiplier $M(t)$, where t is a dimensionless optical depth parameter. The full form of $M(t)$ is a measure of the overall strength of the wind at a given optical depth. For both limiting cases discussed above, we found a marked flattening of the $M(t)$ curve, similar to the flattening of the force multiplier shown in Figure 4 of Lattimer & Cranmer (2021).

https://doi.org/10.1017/S1743921323002867 Published online by Cambridge University Press

We additionally calculate values of the ionization parameter ξ and mean ionization number $\mathcal{I}$ for each model. ξ is defined by the hydrogen ionizing luminosity L_X, the distance from the source r, and the hydrogen number density n_H. ξ and $\mathcal{I}$ are given by

$$\xi = \frac{L_X}{n_H r^2} \quad \text{and} \quad \mathcal{I} = \frac{\sum_i (n_{ion}/n_{el}) i - 1}{Z}, \tag{2}$$

where Z is the atomic number, i is the ionization state, and n_{ion}/n_{el} represents the fractional abundance of each ion of a given element. From our calculations, we found that multiple values of the mean ionization state of the wind material are possible for the same value of ξ. This suggests that ξ is not a complete description of the ionization state of the wind.

3. Future Work

Lattimer & Cranmer (2021) found that a similarly flattened $M(t)$ curve for a wide range of massive stellar models led to a significant quenching of the stellar wind, as well as a quenching of the wind mass-loss rates. The future of this work involves investigating whether the observed $M(t)$ curve will have a similar affect on the mass-loss rates from the AGN accretion disk. Additionally, work on a self-consistent geometry to represent the attenuation of the three luminosity components is already underway. We also plan to explore alternative methods to the ionization parameter ξ, in order to obtain an more accurate and complete picture of the outflow ionization balance.

References

Castor, J. I. 1974, *MNRAS*, 169, 279.
Castor, J. I., Abbott, D. C., & Klein, R. I. 1975, *ApJ*, 195, 157.
Cavaliere, A., Lapi, A., & Menci, N. 2002, *ApJ* (Letters), 581, L1.
Cunto, W. & Mendoza, C. 1992, *Rev. Mexicana AyA*, 23, 107
Cunto, W., Mendoza, C., Ochsenbein, F., et al. 1993, *A&A*, 275, L5
Del Zanna, G., Dere, K. P., Young, P. R., et al. 2021, *ApJ*, 909, 38.
Dere, K. P., Landi, E., Mason, H. E., et al. 1997, *A&AS*, 125, 149.
Fabian, A. C. 2012, *ARAA*, 50, 455.
Giustini, M. & Proga, D. 2019, *A&A*, 630, A94.
Harrison, C. M., Costa, T., Tadhunter, C. N., et al. 2018, Nature Astronomy, 2, 198.
Higginbottom, N., Proga, D., Knigge, C., et al. 2014, *ApJ*, 789, 19.
Hillier, D. J. 1990, *A&A*, 231, 116
Hillier, D. J. & Miller, D. L. 1998, *ApJ*, 496, 407. doi:10.1086/305350
Hillier, D. J. & Lanz, T. 2001, Spectroscopic Challenges of Photoionized Plasmas, 247, 343
Hopkins, P. F., Torrey, P., Faucher-Giguère, C.-A., et al. 2016, *MNRAS*, 458, 816.
King, A. & Pounds, K. 2015, *ARAA*, 53, 115.
Kramida, A., Yu. Ralchenko, Reader, J., & NIST ASD Team. 2018, NIST Atomic Spectra Database (ver. 5.6.1) [Online]. Available: https://physics.nist.gov/asd
Lattimer, A. S. & Cranmer, S. R. 2021, *ApJ*, 910, 48.
Magorrian, J., Tremaine, S., Richstone, D., et al. 1998, *AJ*, 115, 2285.
Mendoza, C., Bautista, M. A., Deprince, J., et al. 2021, Atoms, 9, 12.
Murray, N., Chiang, J., Grossman, S. A., et al. 1995, *ApJ*, 451, 498.
Nomura, M., Ohsuga, K., Takahashi, H. R., et al. 2016, *PASJ*, 68, 16.
Ostriker, J. P., Choi, E., Ciotti, L., et al. 2010, *ApJ*, 722, 642.
Proga, D., Stone, J. M., & Kallman, T. R. 2000, *ApJ*, 543, 686.
Proga, D. 2007, *ASP-CS*, The Central Engine of Active Galactic Nuclei, 373, 267.
Proga, D. & Kallman, T. R. 2004, *ApJ*, 616, 688.
Rees, M. J., Netzer, H., & Ferland, G. J. 1989, *ApJ*, 347, 640.
Risaliti, G. & Elvis, M. 2010, *A&A*, 516, A89.
Silk, J. & Rees, M. J. 1998, *A&A*, 331, L1.
Zhu, Y., Bu, D.-F., Yang, X.-H., et al. 2022, *MNRAS*, 513, 1141.

https://doi.org/10.1017/S1743921323002867 Published online by Cambridge University Press